High Resolution Mapping of Overheating and Mortality Risk

C Liu[a,*], T Kershaw[a], D Fosas[a], A.P. Ramallo Gonzalez[b], S Natarajan[a], D.A. Coley[a]

[a] Dept. Architecture and Civil Engineering, University of Bath, Claverton Down, Bath, BA2 7AY, UK
[b] Faculty of computer science, University of Murcia, Spain.

Abstract

Both the Paris heat wave of 2003 and recent high-resolution climate change predictions indicate a world where mortality from extreme weather events will increase. Most heat wave deaths occur in buildings, and are driven by the thermal characteristics of the buildings and their local environment. Unfortunately previous work on the topic has ignored such spatial variations by either assuming the climate has little variation over a large area, or using archetypes of buildings from stock models. The latter forgetting that neither building characteristics nor landscape context are uniform over a city, with for example suburbs having a different architecture and shading to the inner city. In this work we use a statistical method combined with a new remote surveying tool to assemble accurate models of real buildings across a landscape then map the spatial variability in overheating and excess deaths now and in the future at a resolution of 5km x 5km. High spatial variation in the risk of overheating and heat-related mortality was found due to the variability of architecture, context and weather. Variability from the architecture and shading context were found to be a greater influence on the spatial variation in overheating than climate variability. Overheating risk was found to increase significantly with heat-related mortality tripling by the 2050s. The method was validated against data collected during the northern hemisphere 2006 hot summer. The maps produced would be a highly useful resource for government in identifying populations of greatest concern when developing policies to combat such deaths.

Keywords

Spatial variability; overheating risk; climate change; overheating map; cities; hot summer.

1. Introduction

Despite international efforts to combat global warming since the Rio Earth Summit in 1992 [1], global surface temperatures are projected to rise by up to 4.8 °C by the end of this century [2]. Such warming increases the risk of overheating in non-air-conditioned buildings; a risk which might be further exasperated by fabric improvements [3]. In August 2003, 14,729 excess deaths occurred in France [4] and 2,139 in England and Wales, due to a severe heat wave, primarily in large urban centres [5]. Interestingly, it was found that the top floor presented a higher risk of heat-related mortality, and lack of home insulation was one of the major risk factors for the excess deaths [6]. This indicates that architectural detail and lack of shading are both risk factors in such mortality.

Unfortunately, many weather events that are currently classed as extreme will become more frequent as a result of climate change. For instance, it is reported that the frequency and duration of heat waves are very likely to increase during the 21st century [2], with the heat wave of 2003 representing a typical

* Corresponding author. Tel: +44 (0) 7577 257812.
E-mail address: C.Liu2@bath.ac.uk (C. Liu).

summer by the 2040s, and heat related deaths tripling by the 2050s [3]. Indeed, it is estimated that human activities have already increased the likelihood of a 2003 type event from one in several thousand to ~1:100 in little over a decade [7]. Looking further into the future, heat related deaths are predicted to increase 5-fold under a medium carbon emission scenario (SERS A1B), by the 2080s [3]. A first step to avoiding such deaths and providing occupants with a comfortable indoor environment is a locally-relevant assessment of overheating risk which takes climate change into account.

There have been several general different assessments of future overheating risk, using dynamic thermal models of buildings and future weather files, and all show that overheating risk is on the rise. [8-21]. Appropriate weather files are the prerequisites for any reliable thermal simulation. These take various forms in various parts of the world, for example Test Reference Years (TRYs) and Design Summer Years (DSYs); however, these are normally on too coarse a spatial grid to be locally accurate [22]. Previous research [23] which simulated indoor environmental conditions for different locations across two regions with varying topography, using weather files at a spatial resolution of 5km found that there are distinct variations in overheating risk with location, especially in regions with large topographic differences. Hence it is possible to conclude that location-specific (future) weather data is required to perform accurate overheating risk assessments of populations. Although Eames*, et al.* [23] used weather files at a high spatial resolution, they failed to take into account any variability in the building characteristics and urban form.

It is well known that the presence and form of surrounding buildings can have a major impact on overheating risk due to mutual shading and radiative exchange [24]. The materials used and the architectural form will also have a considerable impact, particularly the thermal mass and the glazing ratio. Hence an accurate assessment would require building information about a large number of buildings across the study area. It is however, not easy to find sufficient building information containing all the necessary variables required for thermal modelling at a large scale. Examples such as housing surveys [25], energy follow-up surveys [26] and energy efficiency databases [27], etc. provide nationwide building information, but none of these datasets are primarily collected for the purpose of thermal modelling [25]. Hence there is a lack of information regarding building orientation, local shading and glazing ratios [24, 28, 29], i.e. they lack context. This has led to there being very few studies that model a large number of real existing buildings individually; instead representative or archetype models of dwelling types have been used with little to no concern of, for example, the surrounding obstructions or how built form, or density, changes across a region or country [9, 19, 21, 28, 30, 31].

This study focuses on current and future spatial variation in overheating risk and heat-related mortality across a landscape. A new method is developed and then applied to a representative medium-large mid-latitude city with large topographic and density differences, and the results validated against calculated excess mortality from measured temperatures in London during 2006. As mentioned above, the problems for such a large scale overheating risk assessment are lack of detailed building information and unrepresentative weather years. These problems have been solved in this study by modelling a large number of randomly selected real dwellings sitting in their real surroundings and the use of probabilistic Hot Summer Years (pHSYs) [32] at a resolution of 5km. In total, 907 distinct thermal models have each been simulated with 100 pHSYs, resulting in 100 probabilistic projections of overheating risk per dwelling for the current climate i.e. 2020s (2010 - 2039) and a possible future climate scenario for the 2050s (2040 - 2069). Maps of the distribution of the overheating risk and the expected heat-related mortality rate across the study area have then been created.

2. Methodology

Sheffield (53.38° N, 1.47° W) was selected as the study area. Sheffield covers an area of 367.94 km^2 and is the 5th largest city in the UK. There are approximately 553,000 people and 237,000 dwellings in the city [33]. The topography varies greatly from east to west, with a National Park bordering the west of the city. The difference in elevation between the east and west areas is around 200 m. Hence, given a surface temperature lapse rate 0.8 °C/100m [34], there should be approximately a 1.6°C difference in temperature between these two regions. The housing density varies across the study area varies from fewer than 10 units per km^2 to more than 7,000 per km^2 [35].

2.1. Representative weather data

Given sufficient observed hourly weather data from a high spatial resolution network of weather stations and climate projections from either global or regional climate models, it is possible to create future weather data for any location in the world using the morphing methodology [36]. Such localised observed hourly weather data however, is typically not available, so synthetic weather data has to be used, for example the UKCP09 weather generator [37] can produce large amounts of synthetic weather data at a 5 km by 5 km resolution for the current century. The UKCP09 weather generator randomly chooses projections of climate change from probability density functions of possible climate change anomalies, and uses these to perturb weather data from a synthetic control period (1961-1990) [38]. It can generate weather data for three emission scenarios (SRES B1, A1B and A1FI) and seven overlapping 30-year time periods spanning 2010 to 2099, in addition to control data spanning 1961-1990. A downside of such weather generators is that each grid square is treated independently with no consistency in underlying weather patterns between adjacent grid squares. However, it has been shown that the differences caused by random sampling within the UKCP09 weather generator are much smaller than the differences due to other factors such as topography between adjacent grid squares [23]. Furthermore, a comparison of future weather data produced by morphing and the UKCP09 weather generator [39], concluded that simulations with morphed future weather files could underestimate the total overheating hours, but at the same time overestimate peak temperatures, providing further justification for the choice of synthetic weather data over a morphing methodology. (Note, there have been several different approaches [32, 40-44] to constructing future weather files for building simulation using the outputs of the UKCP09 weather generator. A review of these different methodologies can be found in the papers written by Mylona [45] and Liu*, et al.* [32].)

For this study the new probabilistic Hot Summer Years (pHSYs) [32] have been used. There are 100 sets of 30-year period weather data obtained from each run of the UKCP09 weather generator. The one with the hottest summer was selected from the 30-year period. In total, 100 hottest summer years were selected from 100 sets and they are ranked based on the ascending order of warm summers to produce 1st to 100th percentile HSYs. Two metrics were used for identifying the warmth of a summer so that there were two types of pHSYs: one is based on Weighted Cooling Degree Hours (WCDH) (pHSY-1) and the other is based on the Physiologically Equivalent Temperature [46] (pHSY-2). In this paper, pHSY-1 (from now on referred to as pHSY) has been used, as this has been shown to be suitable for assessing the severity of overheating risk [32]. Each run of the UKCP09 weather generator can output 100 sets of equi-probable climate and weather projections and hence 100 pHSYs. For each grid square 100 pHSYs were created for two time periods, the 2020s (2010 to 2039) intended to represent the current hot summer years and the 2050s (2040 to 2069) to represent possible future hot summer years.

The city of Sheffield is covered by eighteen UKCP09 grid squares as shown in Figure 1, whilst grid square 0 is within the city's limits, it contains no dwellings and hence no simulations were performed for grid square 0. Using the SRES A1FI emission scenario, 17 sets of 100 pHSYs (1st to 100th percentile HSYs) were produced for the 2020s and 2050s respectively. In total, 3,400 pHSYs (i.e. 100 pHSYs × 17 grid squares × 1 emission scenario x 2 future time periods) were used for this study. The pHSY represent warm/hot summers but are unlikely to include heat waves with a return period of greater than 15 years, hence they are not extreme. With respect to mean summertime air temperature, in this study the 90th percentile pHSY's represented on average the 98th percentile (15°C), and the 50th percentile pHSY's the 90th (14°C) in an ordered list of the weather files used to assemble them in each grid square. With respect to maximum mean three-day air temperature, the 90th percentile pHSY's represented the 94th percentile on average (25°C), and the 50th percentile pHSY's the 77th (24°C).

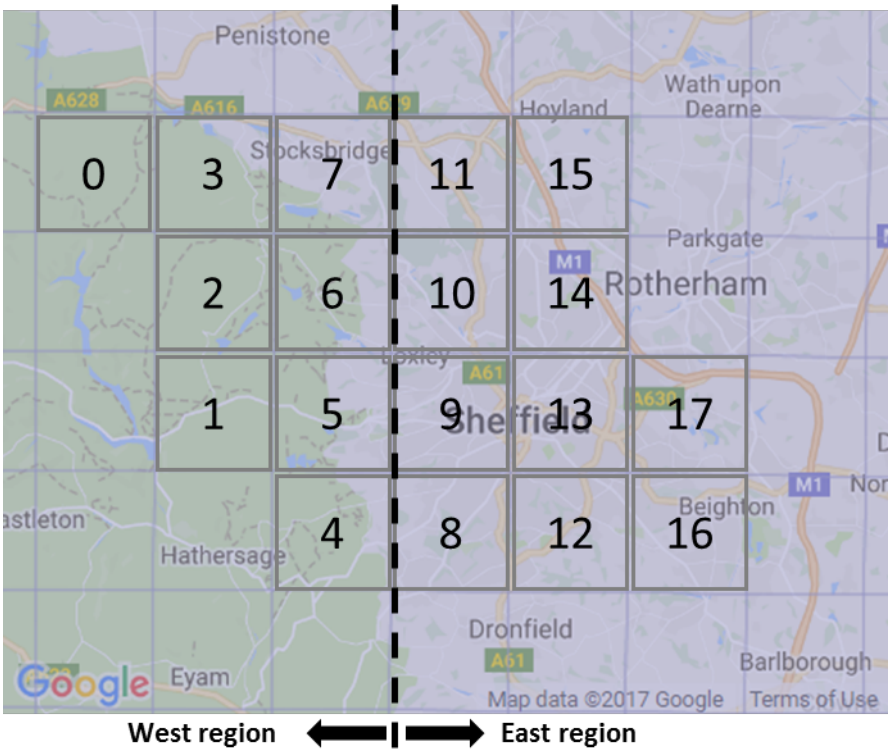

Figure 1. Numbered UKCP09 grid squares for the city of Sheffield [47][1].

2.2. Building information and local shading measurements

In order to assess the fraction of overheated dwellings across the city, the number of dwellings and their form in each grid square was found. Residential areas were derived from Google Maps ® while the existing housing density was found in the report by URBED [35] obtained from Sheffield City Council. The number of dwellings is shown in Figure 2, note the significant difference in the number of dwellings between west (i.e. grid numbers 1 to 7) and east (i.e. grid numbers 8 to 17).

[1] The underlying map of Sheffield was captured from the interactive map of UKCP09. The user interface of which links to Google Maps.

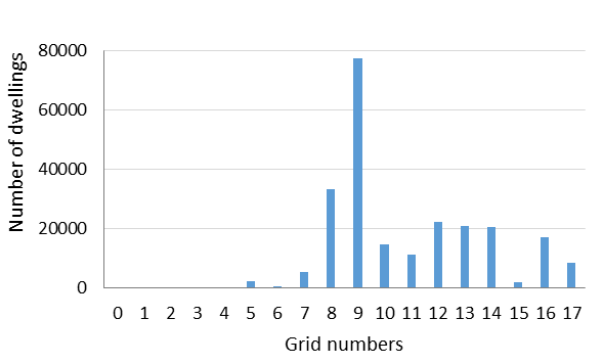

Figure 2. Number of dwellings in each UKCP09 grid square

In order to gather the required detailed building information the survey tool of [48] was used. This tool utilises Google Street View® with Google Maps® so is applicable worldwide. The tool can be used to obtain window sizes and type (i.e. single or double), frame ratio and opening types (awning, casement, slider, hopper etc.), building type, orientation, local shading (i.e. angle of visible sky [49]) and (with human input) wall types (i.e. solid or cavity wall [50]).

It would be infeasible to use the survey tool to garner the information needed to accurately model each of the 237,000 dwellings in the study area, so a random sample of buildings was selected in each grid square. The sample size used is shown in Table 1; note there are only a few rural houses in grid squares numbers 1 to 4 which are located within the National Park (see Figure 1 and Figure 2); in these cases all houses were assessed. The sample size S was found using equation (1) [51]:

$$S = \frac{X^2 \cdot n \cdot p \cdot (1-p)}{ME^2 \cdot (n-1) + X^2 \cdot p \cdot (1-p)} \quad (1)$$

where X^2 is found in a chi-square table for 1 degree of freedom with a given confidence level, n is the population size, p is the population proportion (%) and ME is the desired margin of error (%). The value of p is 0.5 which makes the maximum S [52]. Given a confidence level of 90% and an ME of 10%, S for n between 50,000 and 264,000,000 is 68 which has been used for grid numbers 5 to 17. Using the survey tool five common gross UK dwelling types, i.e. detached houses, semi-detached houses, mid-terrace houses, (top floor) flats and bungalows were identified within the 907 stochastic dwelling measurements. The sample size and the distribution of each dwelling type across the whole study area is shown in Table 1.

Table 1. Sample size and distribution of each dwelling type across the seventeen grid squares

Grid numbers	1	2	3	4	5	6	7	8	9	10	11	12	13	14	15	16	17	In total
Sample size	4	2	10	7	68	68	68	68	68	68	68	68	68	68	68	68	68	907
Detached (%)	1	1	2	1	13	11	10	9	4	8	7	3	2	3	9	12	4	100
Semi-detached (%)	0	0	1	0	6	9	7	8	5	8	6	9	7	9	7	8	11	100
Terraced (%)	0	0	1	0	1	3	10	7	18	8	8	7	13	10	5	4	6	100
Flat (%)	0	0	0	0	10	2	0	7	14	5	5	20	17	8	3	5	3	100
Bungalow (%)	1	0	0	6	13	8	6	6	2	7	14	2	3	3	16	6	6	100

2.3. Thermal modelling

Thermal models of the dwellings found, were created using DesignBuilder v4.2 with additional details from BEPAC Technical Note [53]. These building geometries were augmented with the surrounding obstructions to represent local shading, to create thermal models of 907 distinct dwellings in realistic settings. Since only the main façade of a dwelling is available from the survey tool in many cases, the windows on the other façades were predicted from the fenestration ratio of the measured values compared the ones recommended by the BEPAC Technical Note. Window opening types and glazing type were assumed to be consistent between the front and the rear of the dwelling. The images from the survey tool served to identify wall types i.e. solid or cavity wall but not wall insulation, which was estimated using the English Housing Survey Headline Report 2014-15: i.e. that 69% of the cavity walls were insulated while only 9% of the solid walls were insulated [54]. The three predominant constructions used in the thermal modelling were: (1) solid walls with single glazing and wooden frame windows, (2) uninsulated cavity walls with single glazing and wooden frame windows, and (3) insulated cavity walls with double glazing and uPVC frame windows. Details of constructions and derived thermal properties can be found in the online supplementary material [55]. Living rooms were assumed to be occupied between 9 a.m. and 10 p.m., while bedrooms were occupied between 11 p.m. and 8 a.m., based on the national overheating risk survey [56]. The number of occupants was assumed to be the number of bedrooms plus one assuming that two people occupy the main bedroom, with a single occupant for all other bedrooms [57]. UK dwellings are typically not air conditioned, utilising natural ventilation for cooling during hot weather. Window opening was triggered in the models when (1) the internal temperature (T_{in}) > 24°C and (2) T_{in} > the external temperature (T_{ex}) and (3) only during occupied hours. In the simulations the aerodynamic opening area of the windows has been set to 20% of the total openable area. Internal gains from people, equipment, lighting, etc. were assumed to be 3.9 W/m^2 and 3.58 W/m^2 for living rooms and the main bedrooms respectively [58].

2.4. Overheating risk assessment

The indoor thermal environment was assessed over the summer period from April to September using four metrics: (i) mean operative temperature, (ii) average daily maximum operative temperature, (iii) percentage of occupied hours above the threshold operative temperatures i.e. 28°C for the living room and 26°C for the bedroom, and which should be no more than 1% over the year [59], and (iv) Weighted Cooling Degree Hours (WCDH) [60]. Hours of overheating was used to identify the number of overheated dwellings while WCDH was used to measure the severity of overheating.

In addition to the above metrics, the risk to human life from overheating was also estimated based on the methodology proposed by Armstrong*, et al.* [61]. Armstrong*, et al.* [61] found that excess summer deaths are strongly associated with the summertime 2-day mean external temperature (T_{2-day}^{mean}), with the relative risk of death increasing linearly above a threshold temperature. This threshold temperature was shown to be coincident with the 93rd percentile of T_{2-day}^{mean} for all regions investigated [61]. Thus the heat-related mortality (M) for a summer was calculated from the relative risk (RR) given by:

$$M = D_{summer}^{all-cause} \cdot (RR - 1) \quad (2)$$

with

$$D_{summer}^{all-cause} = \frac{d}{365} \cdot D_{year}^{all-cause} \quad (3)$$

and

$$RR = \alpha \cdot T_{2-day}^{mean} + \beta, \quad (4)$$

where $D_{summer}^{all-cause}$ is the deaths over the summer from all causes, $D_{year}^{all-cause}$ the deaths in one year from all causes, and d is the number of days when the T_{2-day}^{mean} is above the threshold temperature identified for heat-related mortality. RR is the relative risk, a linear relationship between external temperature and mortality; α is the heat-mortality slope in % per degree above the mortality threshold temperature. The external mortality threshold temperature for Sheffield has been shown to be 22.2°C with α equal to 1.7% [61]. β can be calculated when RR equals 1 and T_{2-day}^{mean} is equal to the mortality threshold temperature. For this paper, which considers the spatial overheating risk across a city and for different dwelling types, external temperature is not an ideal indicator of the relative risk of mortality, instead it is preferable to use an internal mean temperature. To calculate the mortality rates for this study we have assumed that the mortality threshold temperature will occur at the 93rd percentile of internal 2-day mean temperatures, as it does externally. For each of the 17 grid squares the 100 HSY files were ranked in order to obtain the 93rd percentile of external T_{2-day}^{mean}. By choosing like percentiles from each grid square (i.e. median HSY from grids 1, 2, 3, etc.) the equivalent internal mortality threshold temperature was identified for each of the 907 dwellings (using living room temperatures for daytime and bedroom temperatures for night-time) and the average was taken to produce a citywide internal mortality threshold. In this way 100 citywide mortality thresholds were created to allow the probabilistic assessment of the relative risk. Population and $D_{year}^{all-cause}$ information was extracted at Middle Layer Super Output Area (MSOA) data from the UK Office for National Statistics (ONS) [62]. However, MSOAs do not match up with the UKCP09 grids, hence RR for each MSOA was adjusted based upon the proportion of the MSOA within each UKCP09 grid square.

3. Results and discussion

3.1. Variability in the external environment

External mean (T_{mean}^{ex}) and average daily maximum temperature (T_{max}^{ex}) over the summer (April to September) were calculated for the 100 pHSYs (i.e. 1st to 100th percentile HSYs) for each grid square for the 2020s (which is intended to represent the current climate). The variation of T_{mean}^{ex} and T_{max}^{ex} across the city is shown in Figure 3. The median values (red line in the box plot) of T_{mean}^{ex} and T_{max}^{ex} were found to have a variance of 0.40 and 0.61 respectively. The largest differences for the median values of T_{mean}^{ex} and T_{max}^{ex} among the seventeen grids were 2.8°C and 3.1°C respectively. In addition, median T_{mean}^{ex} and T_{max}^{ex} in the western region (grid numbers 1 to 7) were 1.6°C and 1.9°C lower than the eastern region (grid numbers 8 to 17). Given the difference in temperature between adjacent grid squares is up to twice as much as that indicated by the surface temperature lapse rate, it is clear that lapse rate alone is not a good way to account for variations in temperature across the landscape when considering overheating. Regarding the variation from 100 pHSYs within each grid, the variances of T_{mean}^{ex} and T_{max}^{ex} were approximately 0.4 and 0.6°C^2 respectively, which are consistent for all of the seventeen grids.

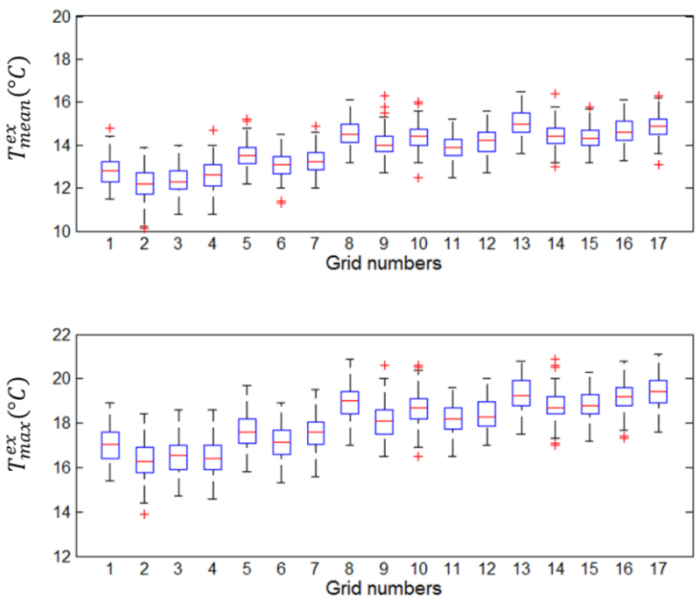

Figure 3. External mean and average daily maximum temperatures over the summer period (April to September) for the 2020s.

3.2. Variability in the indoor thermal environment

Across the 17 grid squares, 907 dwellings were simulated using a high performance computing environment for 100 pHSYs, resulting in 90,700 simulations for each time period. As might be expected from the external temperature, the indoor environment in the eastern region was warmer than the western region (Figure 4). On average, the difference in T^{in}_{max} between the two regions was 1.8°C for the living rooms and 1.4°C for the main bedrooms. The variability in T^{in}_{max} between the 17 grid squares however was up to 3.9°C for the living rooms and up to 3.1°C for the main bedrooms. The variances of T^{in}_{max} across the 17 grid squares were 1.0 and 0.75°C^2 for the living rooms and the main bedrooms respectively, i.e. higher than the variance of T^{ex}_{max} shown in Figure 3. For each grid square, there was greater variation in T^{in}_{mean} and T^{in}_{max} than in T^{ex}_{mean} and T^{ex}_{max}, suggesting variability does arise from the way the spectrum of dwelling types and their context varies over the study area, in addition to the weather.

Figure 5 shows a comparison between median internal operative temperatures (i.e. T^{in}_{mean} and T^{in}_{max}) for the 2020s and 2050s. For both the living room and the main bedroom the differences in median internal temperatures (ΔT, see secondary y-axis in Figure 5) between the 2020s and 2050s was < 1°C over the summer for all seventeen grid squares. In addition, the distribution for the 2050s was very similar to that for the 2020s indicating that the distribution in overheating risk is unlikely to change substantially due to a changing climate.

In summary, due to a combination of their architecture, their context and their location the dwellings in the eastern region are at a higher overheating risk than those in the western region and will remain so in future. This suggests that any policies should preferentially consider the population living in this area. In addition, the largest absolute difference of internal temperature (3.9°C) between grid squares is approximately twice as much as the difference (1.6°C) in external temperature from a consideration of surface temperature lapse rate alone. Thus it is clear any variations in external temperature caused by the lapse rate across a region should not be seen as indicative of internal temperature differences across the region. This conclusion, which suggests that overheating assessments must take into

account of how the architecture and shading context changes across a region supports previous work [63]. This showed that the increase in internal temperature due to a changing climate was very much dependent on built form. With some buildings increasing in mean and maximum temperature faster than any changes in external temperature, and some less rapidly than the external perturbation.

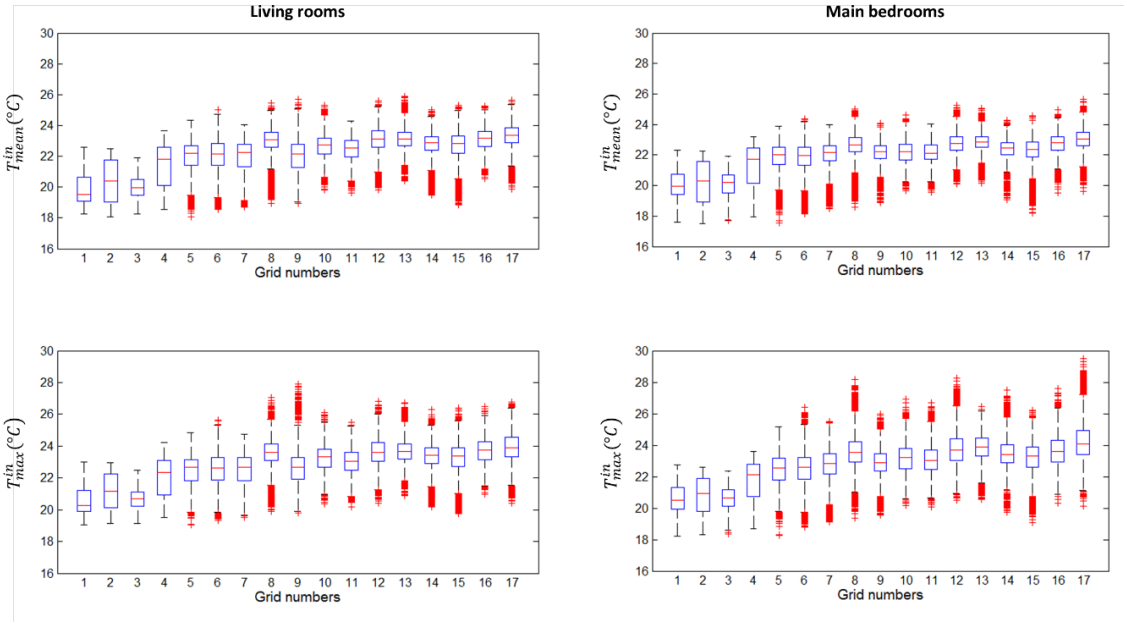

Figure 4. Internal mean and average maximum operative temperatures during the summer (April to September) in the 2020s.

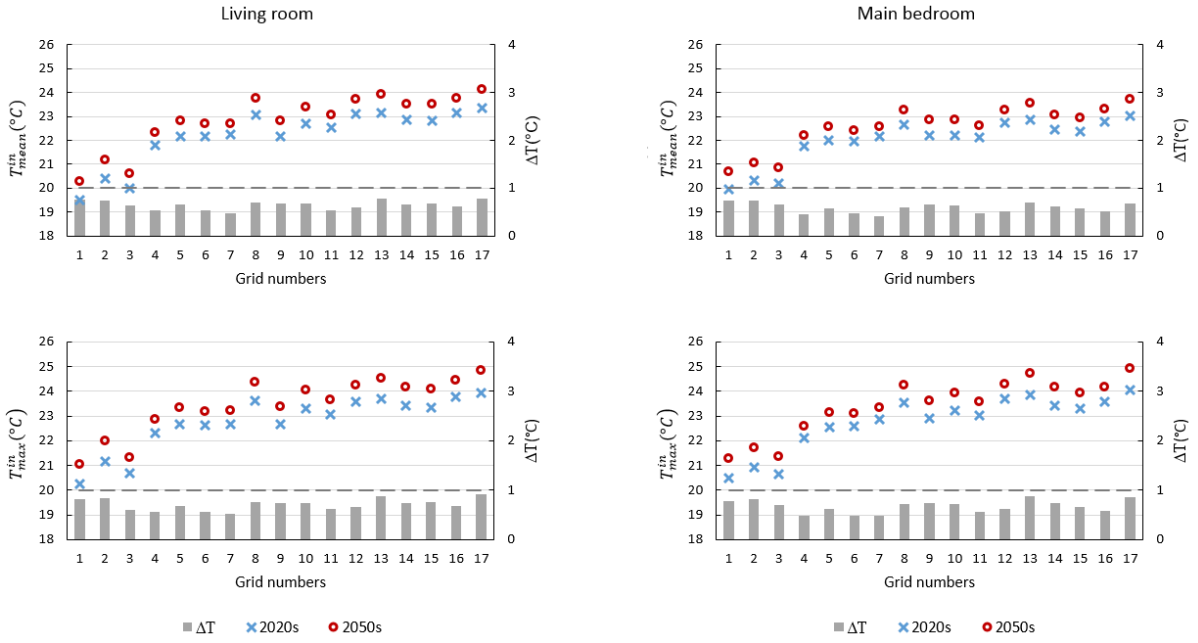

Figure 5. Variation in the median T^{in}_{mean} and T^{in}_{max} across the city in the 2020s and in 2050s. ΔT shows the increase in T^{in}_{mean} (or T^{in}_{max}) by the 2050s compared to the 2020s.

As mentioned above, 907 thermal models of dwellings were simulated with 100 pHSYs, resulting in 100 probabilistic projections of overheating risk per dwelling, or 90,700 predictions in total. The median (50th percentile) projection of overheating for each of the 907 dwellings, sorted by type for all four overheating metrics considered, is shown in Figure 6. The method used, which is based on real survey data and shading, allows for a much more accurate consideration of which architectural forms are more at risk of overheating than work based on archetypes. It accounts for example for the observation (confirmed by the survey tool) that the lower floors of terrace housing in the urban environment is more likely to be shaded by other properties than detached homes in the suburbs. Comparisons between dwelling types indicate that, living rooms in the semi-detached houses, flats and bungalows, and bedrooms in the semi-detached and terraced houses are likely to be at a higher risk of overheating. Overall, detached houses were the coolest dwelling type which is consistent with results from previous work [56]. Top floor flats showed the highest overheating risk for living rooms (see Figure 6); this also agrees with the same reference. By contrast, for terraced houses overheating risk was lower in the living rooms compared to the bedrooms. Table 2 shows the percentage of overheated living rooms and bedrooms for each dwelling type for both 2020s and the 2050s. The number of overheated living rooms is projected to double by the 2050s compared to the 2020s, while the number of the overheated bedrooms is projected to increase dramatically by the 2050s.

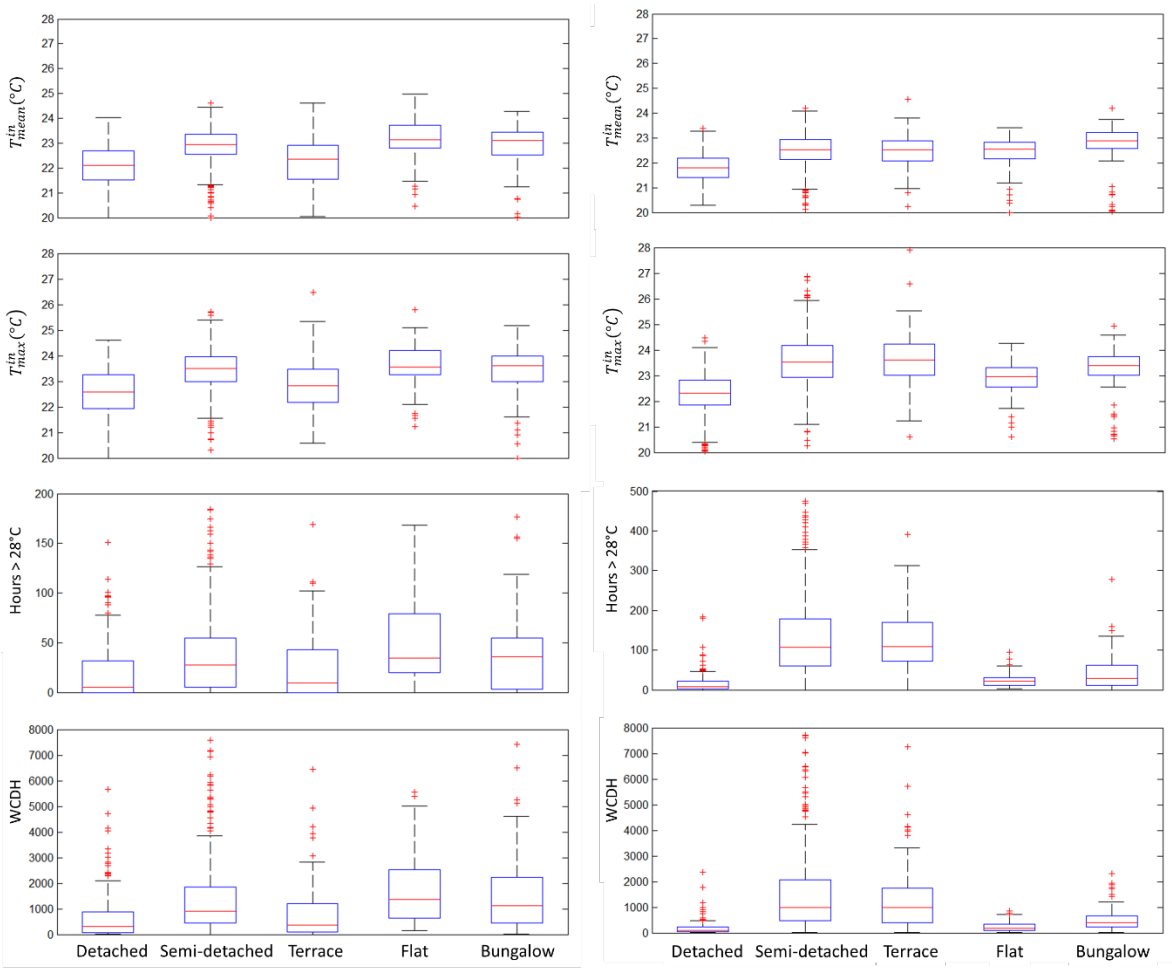

Figure 6. Variability in overheating for the different metrics for different dwelling types (living rooms on left; main bedrooms on right).

Table 2. Percentage of overheating dwellings, shown by dwelling type, data shown at the 50th percentile (Median). N is the number of samples.

Periods	Rooms	Detached (N=185)	Semi-detached (N=400)	Terraced (N=177)	Flat (N=59)	Bungalow (N=86)
2020s	Living room	18.4%	31.0%	18.1%	44.1%	33.7%
	Bedroom	0.0%	7.5%	44.6%	1.7%	8.1%
2050s	Living room	45.9%	69.8%	50.8%	88.1%	70.9%
	Bedroom	5.4%	42.3%	97.7%	42.4%	46.5%

3.3. Maps of overheating risk

Maps of overheating were created, detailing both the number of overheating dwellings (based on hours of overheating) and the severity of overheating (based on WCDH) (Figure 7). The size of a circle illustrates the number of overheated dwellings while the colour displays the severity of the overheating risk. The number of the overheated dwellings in each grid square was estimated from the percentage of overheated samples and the actual number of dwellings shown in Figure 2. WCDH is found to increase by 50% for the living rooms and 19% for the main bedrooms for the 2050s compared to the 2020s.

There is a significant difference in the risk and severity of overheating between grid squares and between the eastern and western regions. This can be attributed not only to the higher external temperatures on the east side of the city but also the increased number of dwellings. On the west side of the city, only 3% of living rooms overheated in the 2020s rising to 16% by the 2050s (median estimate). While on the east side of the city overheating of living rooms was 34% and 74% for the 2020s and 2050s respectively. With respect to bedrooms, the east of the city showed approximately three times the risk than the west. The maps illustrate the high variability of both the overheating risk to dwellings and the severity of the overheating across the city.

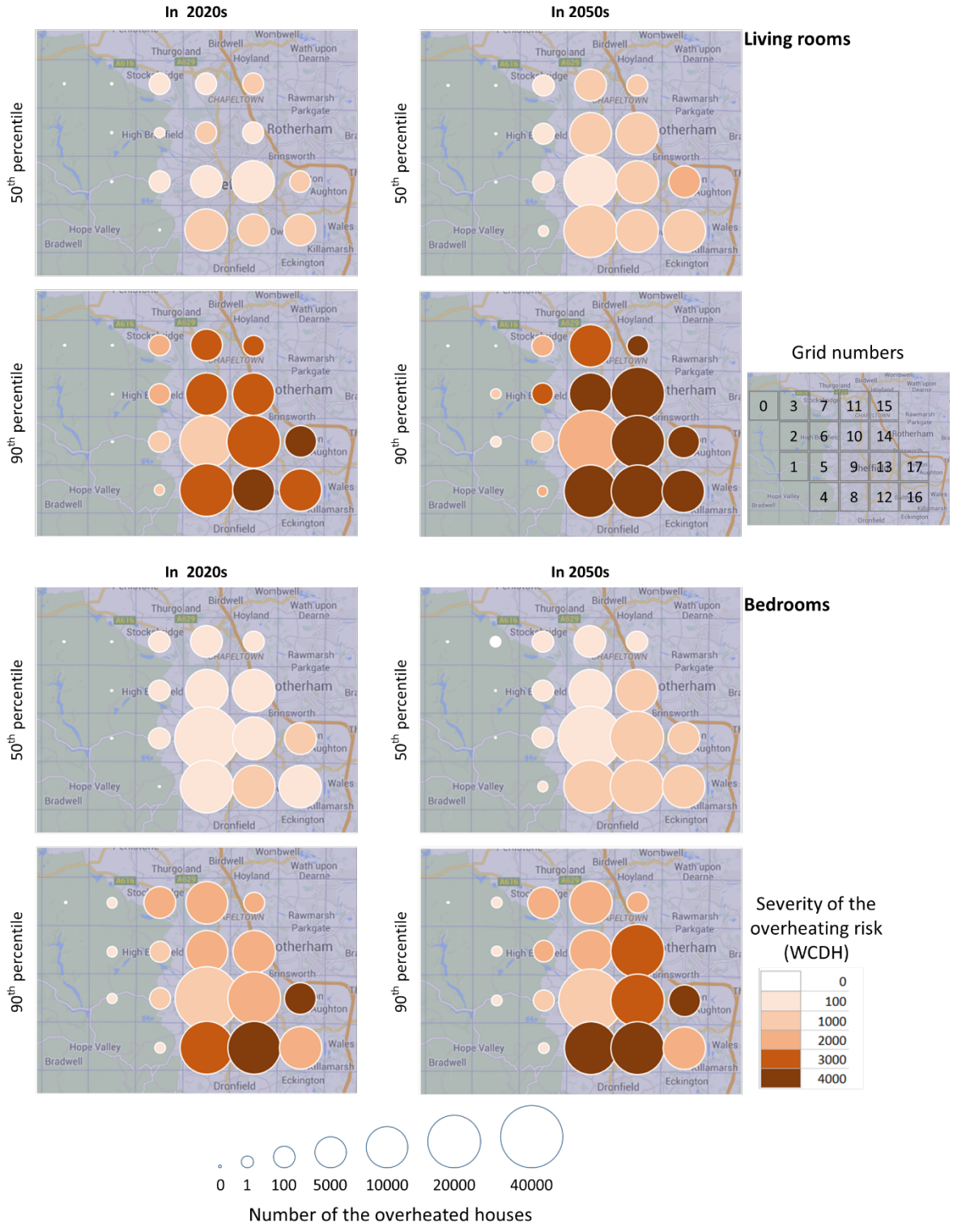

Figure 7. Overheating risk maps for the study area for the 2020s and 2050s. The size of the circle represents the number of overheating dwellings exceeding 1% of annual occupied hours above a set temperature. The colour scale represents the severity of the overheating risk measured by the number of WCDH.

3.4. Spatial variability of overheating risk

We have seen that the risk and severity of overheating varies with both location and architecture/context. This section examines which has the greater impact.

Within each pane, variability in T^{in}_{mean}, T^{in}_{max}, hours of overheating and WCDH are shown in Figure 8 and Figure 9. Variability in the weather between different grid squares is shown on the left; while variability between different samples of a single dwelling type is shown on the right.

In order to assess the variations in the overheating risk due to the spatial variability in the localised weather, two thermal models for each dwelling type were simulated with all of the weather files from across the city. The two thermal models were selected as follows: all the buildings within each dwelling type were ranked in order of overheating risk in the living room and the median model was selected; the other one was selected in the same way but based on the overheating risk in the main bedroom. Each model was simulated using 100 pHSYs for each grid square and the median result for each overheating metric was used to create the left-hand box plots. To assess the variability of different dwellings, all the thermal models within the same dwelling type were simulated with 100 pHSYs for the same location (weather data for grid square 9 was used, as this has the highest housing density and is in the middle of the city). For each dwelling model the median value of each overheating metric was used to create the right-hand boxplot. In summary, we are moving one building (the median one) of each basic type around the city and studying the variation in overheating found; and also placing all the buildings of the same type into one grid square to also look at the variation found. This allows a comparison in the variance due to weather to be compared to the difference caused by architecture and context.

As shown in Figure 8 and Figure 9, the interquartile ranges (IQR) of $T^{in}_{mean}$and T^{in}_{max} (left-hand box plots) for all dwelling types are similar. We can also see from Figure 8 and Figure 9 that the IQR of T^{in}_{mean} and T^{in}_{max} for inter-dwelling type variability (right-hand box plots) is roughly double the IQR variability (left-hand box plots) due to localised weather variability. This increased inter-dwelling type variability is carried over into the plots for hours of overheating and WCDH. The IQR of the hours of overheating and WCDH is shown to be up to 56 and 2150 for the living rooms and 101 and 1591 for the main bedrooms. In addition, the inter-dwelling type plots have a significantly greater range, highlighting the importance of the local setting on both overheating risk and severity. Such variability implies that it may be more appropriate to present a likely range of overheating risk based on a number of samples for a dwelling type rather than a single archetype model which may well show significantly biased results. The spatial variability in the localised weather also has a significant impact on the likely range of overheating risk, albeit to a lesser extent than the local context. The IQR of the hours of overheating and WCDH due to the variability in the weather, were in excess of 20 hours and 400 for the living rooms for all dwelling types and over 60 hours and 800 for the main bedrooms of semi-detached and terraced houses. The spatial variability in the weather therefore should be taken into consideration when completing risk assessments, though its influence was not as great as the variability in the dwellings.

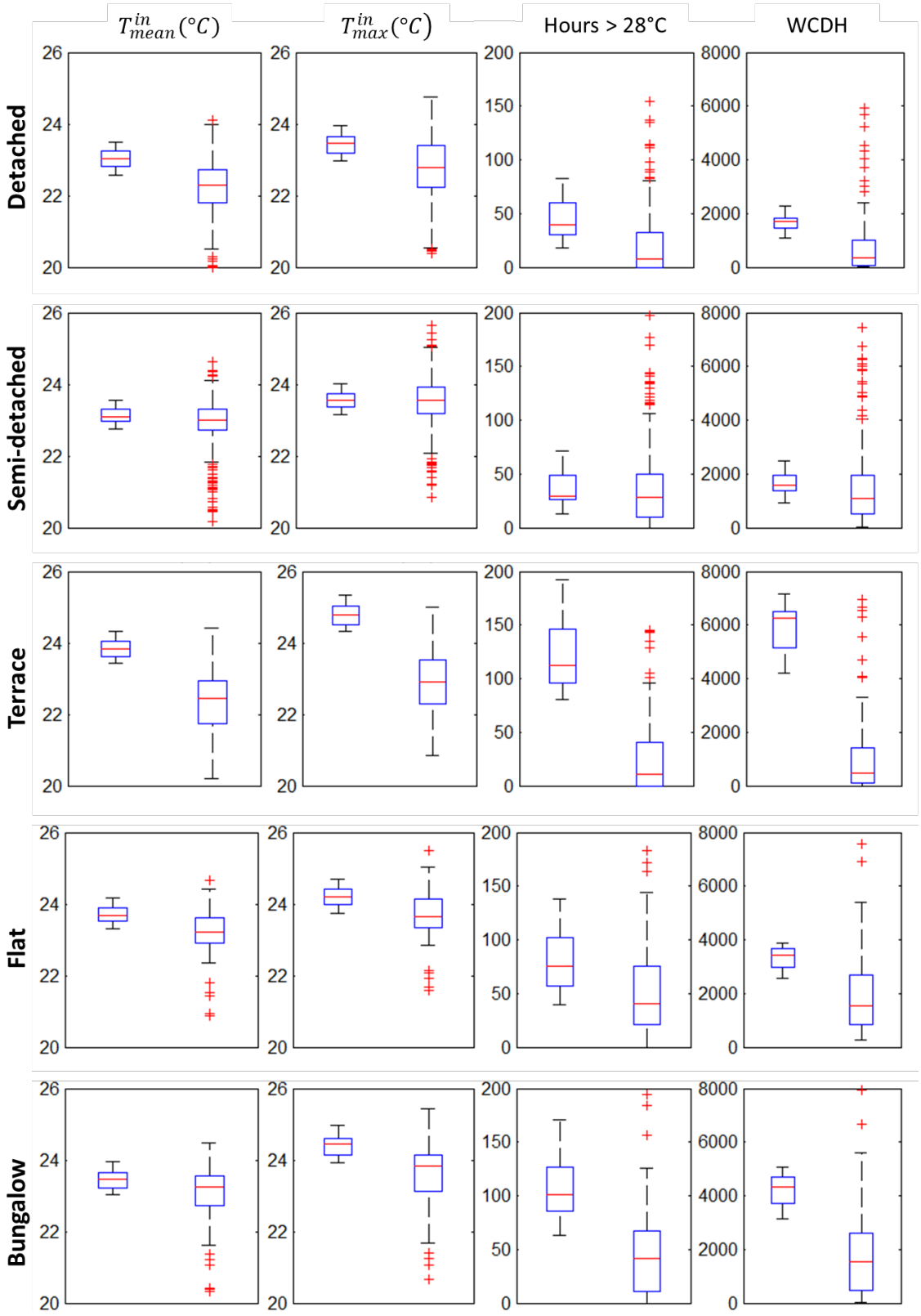

Figure 8. Comparison between the influence of variability of localised weather and dwellings for different overheating metrics within living rooms. The left-hand boxplot in each cell shows the variation caused by the spatial variability in the weather across the seventeen grids squares while the right-hand boxplot shows the variation given by all the samples within each dwelling type, but for a single grid square—i.e. the variability due to the architecture and context.

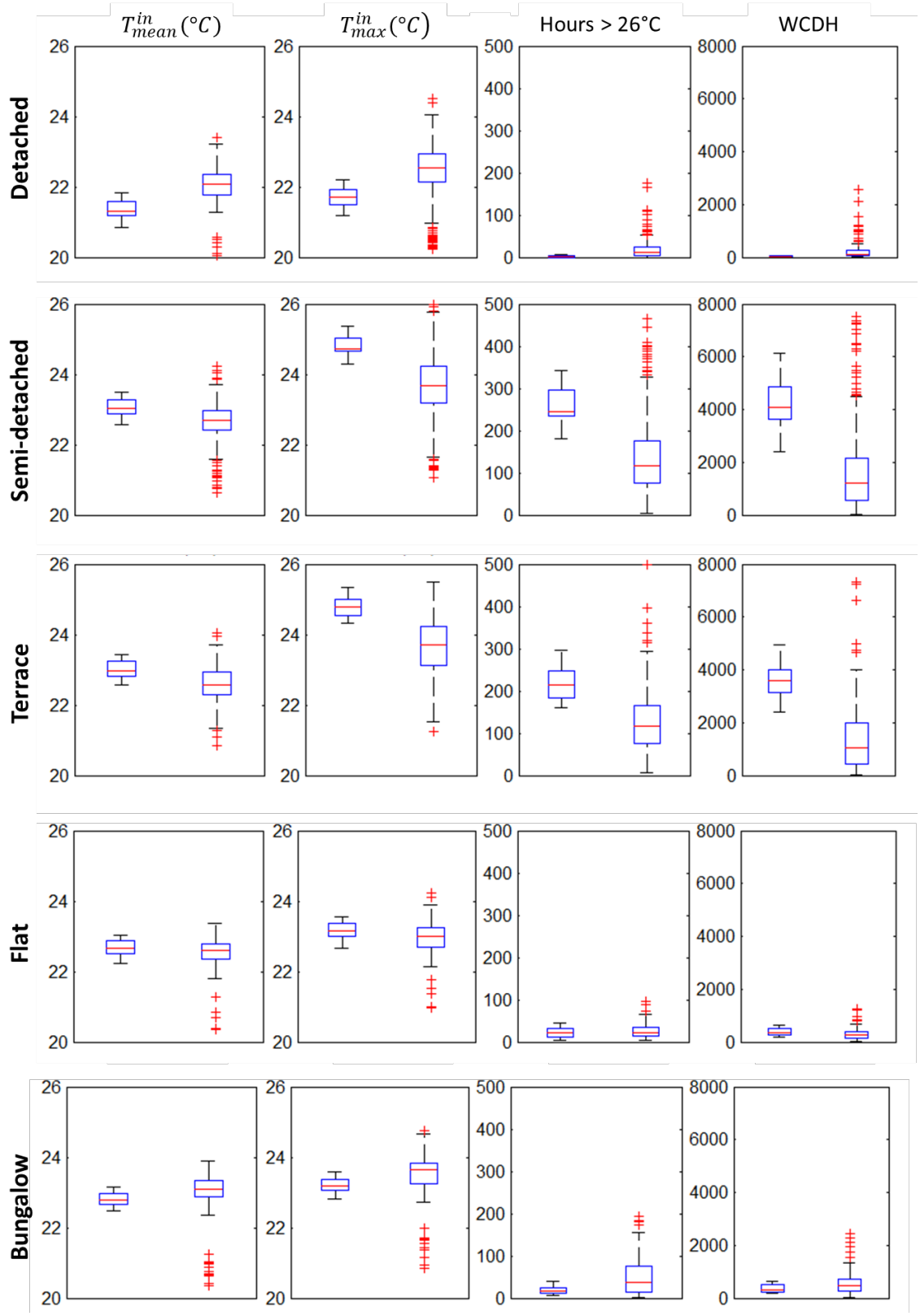

Figure 9. Comparison between the influence of variability of localised weather and dwellings for different overheating metrics within main bedrooms. The left-hand boxplot in each cell shows the variation caused by the spatial variability in the weather across the seventeen grids squares while the right-hand boxplot shows the variation given by all the samples within each dwelling type, but for a single grid square—i.e. the variability due to the architecture and context

3.5. Validation and heat-related mortality at a sub-city level

As stated in the methodology, the mortality M is determined from the linear relationship between relative risk and the internal 2-day mean temperature (T_{2-day}^{mean}) above a citywide mortality threshold temperature. From the latest population and $D_{year}^{all-cause}$ data available at the MSOA (ward) level [62], the heat-related mortality rates (M) in deaths/million over the summer (April to September) were estimated.

It is currently unclear at what rate people may adapt to higher temperatures as the climate changes. If people do not adapt quickly the mortality threshold temperature for the 2050s will be similar to the 2020s. Therefore, two maps have been produced for the 2050s, one where the 2020s mortality threshold has been used to calculate M and one where a new threshold temperature has been calculated to represent full adaptation to a warmer climate. The citywide mortality thresholds were calculated as 24.4°C and 25.9°C for the 2020s and 25.4°C and 27.2°C for the 2050s at the 50th and 90th percentiles respectively. The 50th and 90th percentile projections of M for the 2020s are 7 and 12 per million per year respectively, increasing to 21 and 39 per million per year in the 2050s in the absence of any adaptation (using the 2020s mortality threshold). Thereby indicating that the heat-related mortality rate would triple in a 30-year period if people were unable to adapt to a warming climate.

By using pHSYs this work is predicated on warmer than average summers and hence overestimates risk during colder summers. However, the weather generator [37] that lies behind the pHSYs is not designed to produce heat waves or other rare events with long return periods. The pHSY is designed to solve this difficulty of needing to ensure overheating risk is not underestimated by using only typical years, but recognising there being (as yet) no robust way of generating accurate heat waves with accurate return periods across a landscape. The approach was validated by considering data from the hot summer of 2006. During May to August in 2006 (which included a 4-day hot spell) M for London was estimated (based on the recorded temperatures) as 33.5 per million (14.2 per million during one 4-day spell) [31]. So, with the 90th percentile projection for 2050s, Sheffield would experience yearly heat-related mortality similar to that found for London during the hot summer in 2006.

The mortality rate shown at a ward level across the city of Sheffield shows similar spatial variation to the overheating displayed in Figure 7, with the eastern region showing significantly greater heat-related mortality rates than the western region. Also variation between regions is more pronounced in the 2050s compared to the 2020s. The variances for the 50th and 90th percentile M are 21 and 79 for the 2020s but 142 and 403 for the 2050s.

If people do adapt quickly to the warming climate (using the threshold temperatures of mortality for the 2050s), the 50th and 90th percentile projections of M for the 2050s are 6 and 16 per million which are quite similar to the M of the 2020s suggesting that the adverse impact of the warming climate on M could be offset by human thermal adaptation. Also the spatial variation does not change as the variances for the 50th and 90th percentile M are 18 and 80, i.e. similar to those of the 2020s. Figure 10 shows M at a ward level, for the 2020s and 2050s at the 50th and 90th percentiles for both levels of adaptation.

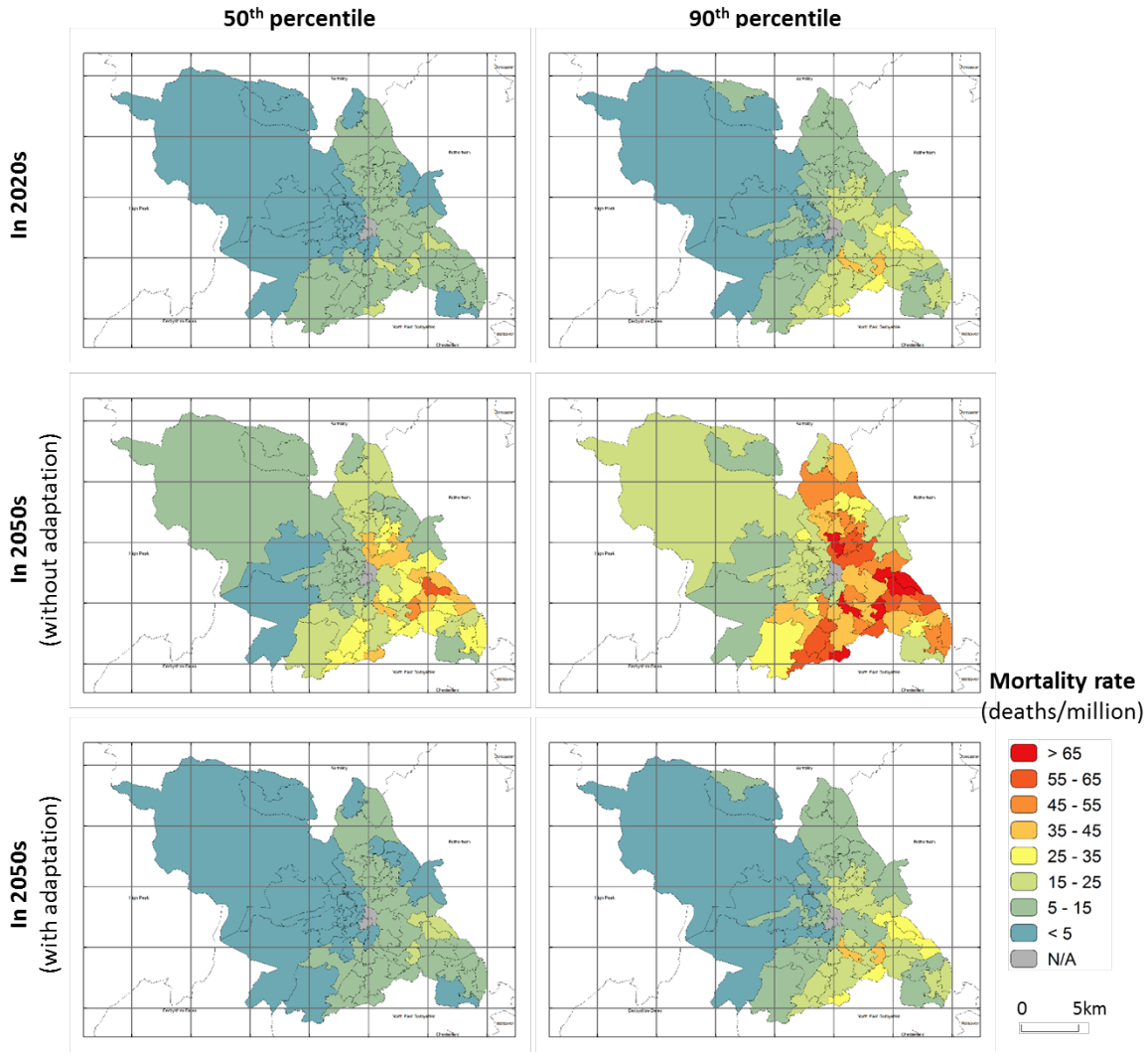

Figure 10. Heat-related mortality rates (deaths/million) for the 2020s and 2050s. The mortality rates with and without human adaptation to the warming climate are shown for 2050s. Two MSOAs lack death data and are coloured grey. The 5km by 5km UKCP09 grid is overlaid for reference. The population of an MSOA on average is 7,200.

4. Conclusions

In this paper we have developed a new method for mapping the spatial variability of overheating and associated human mortality rates of a city, region or country and validated this against measured data for London. By applying the approach to a medium sized mid-latitude city and its surrounding countryside we have shown that spatial variability is material to the question of overheating assessment, and that much of this variability arises from the way building type varies across a region.

Rather than using a national stock model approach, which might not account for local architectural features, or shading from local street layouts, a robust stochastic approach was used. A remote survey tool [48] was used to gather the details of 907 buildings and their surroundings within seventeen 5km by 5km grid squares. The details included building type, building orientation, shading from the surrounding context, wall types, window types, glazing ratio, opening types and opening area. Each of these 907 dwellings were simulated using dynamic thermal modelling using standard occupancy levels and internal gains and probabilistic localised weather data for the 2020s and 2050s.

Examination of temperatures across the city show a strong correlation between external temperatures and topography. While, variation in T_{mean}^{in} and T_{max}^{in} across the city is more strongly correlated with the type of dwelling. In all cases the inter-dwelling type variability in overheating for all overheating metrics considered is greater than the variability due to weather. This implies that the details of local surroundings and local architecture are an important aspect when considering overheating risk.

Overheating maps have been created which show both the risk of overheating (based upon a number of hours criterion) and the severity of overheating (based upon WCDH). The maps show high spatial variations in both the risk and severity of overheating in dwellings across the city. The eastern side of the city showed overheating risk over three times that of the western side for the 2020s and 2050s. The maps indicate that the number of overheated dwellings and the severity of such overheating will increase substantially by the 2050s in the absence of any building adaptations. Such overheating maps will be a useful resource to identify areas of concern regarding the risk and severity of overheating in dwellings and for developing policy.

The impacts of location and vernacular form are also found to be important when considering heat related mortality, with some areas experiencing a 10-fold greater mortality rate than others.

It is clear from this work that it is critical to consider both the local weather and the local architecture (and its surroundings) when analysing overheating risk and future mortality rates. Doing so will also allow the identification of priority areas for adaptation of buildings, and priority populations, and thereby inform decision making about action plans.

Acknowledgements

We are thankful for the IT serveries of Balena i.e. the High Performing Computing system to execute a substantial number of dynamic thermal simulations.

References

[1] United Nations, United Nations Framework Convention on Climate Change, United Nations, 1992.
[2] IPCC, Climate Change 2013: The Physical Science Basis. Contribution of Working Group I to the Fifth Assessment Report of the Intergovernmental Panel on Climate Change [Stocker, T.F., D. Qin, G.-K. Plattner, M. Tignor, S.K. Allen, J. Boschung, A. Nauels, Y. Xia, V. Bex and P.M. Midgley (eds.)], Cambridge University Press, Cambridge, United Kingdom and New York, NY, USA, 2013.
[3] ASC, UK Climate Change Risk Assessment 2017 Synthesis Report: priorities for the next five years, London, 2016.
[4] A. Fouillet, G. Rey, F. Laurent, G. Pavillon, S. Bellec, C. Guihenneuc-Jouyaux, J. Clavel, E. Jougla, D. Hémon, Excess mortality related to the August 2003 heat wave in France, International Archives of Occupational and Environmental Health 80(1) (2006) 16-24.
[5] H. Johnson, R.S. Kovats, G. McGregor, J. Stedman, M. Gibbs, H. Walton, The impact of the 2003 heat wave on daily mortality in England and Wales and the use of rapid weekly mortality estimates, Euro surveillance : bulletin européen sur les maladies transmissibles = European communicable disease bulletin. 10(7) (2005) 168-171.
[6] S. Vandentorren, P. Bretin, A. Zeghnoun, L. Mandereau-Bruno, A. Croisier, C. Cochet, J. Riberon, I. Siberan, B. Declercq, M. Ledrans, August 2003 heat wave in France: risk factors for death of elderly people living at home, European journal of public health 16(6) (2006) 583-91.
[7] N. Christidis, G.S. Jones, P.A. Stott, Dramatically increasing chance of extremely hot summers since the 2003 European heatwave, Nat Clim Change 5(1) (2015) 46-50.
[8] R.S. McLeod, C.J. Hopfe, A. Kwan, An investigation into future performance and overheating risks in Passivhaus dwellings, Building and Environment 70 (2013) 189-209.
[9] R. Gupta, M. Gregg, Using UK climate change projections to adapt existing English homes for a warming climate, Building and Environment 55(0) (2012) 20-42.
[10] M.F. Jentsch, A.S. Bahaj, P.A.B. James, Climate change future proofing of buildings—Generation and assessment of building simulation weather files, Energy and Buildings 40(12) (2008) 2148-2168.
[11] D.P. Jenkins, S. Patidar, P.F.G. Banfill, G.J. Gibson, Probabilistic climate projections with dynamic building simulation: Predicting overheating in dwellings, Energy and Buildings 43(7) (2011) 1723-1731.
[12] T. Frank, Climate change impacts on building heating and cooling energy demand in Switzerland, Energy and Buildings 37(11) (2005) 1175-1185.
[13] D. Coley, T. Kershaw, M. Eames, A comparison of structural and behavioural adaptations to future proofing buildings against higher temperatures, Building and Environment 55 (2012) 159-166.
[14] C. Demanuele, A. Mavrogianni, M. Davies, M. Kolokotroni, I. Rajapaksha, Using localised weather files to assess overheating in naturally ventilated offices within London's urban heat island, Building Services Engineering Research and Technology 33(4) (2012) 351-369.
[15] K. Jenkins, J. Hall, V. Glenis, C. Kilsby, M. McCarthy, C. Goodess, D. Smith, N. Malleson, M. Birkin, Probabilistic spatial risk assessment of heat impacts and adaptations for London, Climatic Change 124(1) (2014) 105-117.
[16] W. Tian, P. de Wilde, Thermal building simulation using the UKCP09 probabilistic climate projections, Journal of Building Performance Simulation 4(2) (2011) 105-124.
[17] P. Wilde, W. Tian, Identification of key factors for uncertainty in the prediction of the thermal performance of an office building under climate change, Building Simulation 2(3) (2009) 157-174.
[18] P. de Wilde, W. Tian, Predicting the performance of an office under climate change: A study of metrics, sensitivity and zonal resolution, Energy and Buildings 42(10) (2010) 1674-1684.
[19] R. Gupta, M. Gregg, Preventing the overheating of English suburban homes in a warming climate, Building Research & Information 41(3) (2013) 281-300.
[20] A.D. Peacock, D.P. Jenkins, D. Kane, Investigating the potential of overheating in UK dwellings as a consequence of extant climate change, Energy Policy 38(7) (2010) 3277-3288.

[21] A. Mavrogianni, P. Wilkinson, M. Davies, P. Biddulph, E. Oikonomou, Building characteristics as determinants of propensity to high indoor summer temperatures in London dwellings, Building and Environment 55(0) (2012) 117-130.
[22] CIBSE, Future CIBSE TRY/DSY Hourly Weather Data, The Chartered Institution of Building Services Engineers London, 2013.
[23] M. Eames, T. Kershaw, D. Coley, The appropriate spatial resolution of future weather files for building simulation, J Build Perform Simu 5(6) (2012) 347-358.
[24] J.A. Futcher, T. Kershaw, G. Mills, Urban form and function as building performance parameters, Build Environ 62 (2013) 112-123.
[25] DCLG, English Housing Survey TECHNICAL REPORT 2013-14, Department for Communities and Local Government, London, UK, 2015.
[26] DECC, Energy Follow-Up Survey 2011, Department of Energy and Climate Change, London, UK, 2013.
[27] EST, Homes Energy Efficiency Database, Energy Saving Trust, London, UK, 2013.
[28] J. Taylor, M. Davies, A. Mavrogianni, Z. Chalabi, P. Biddulph, E. Oikonomou, P. Das, B. Jones, The relative importance of input weather data for indoor overheating risk assessment in dwellings, Building and Environment 76(0) (2014) 81-91.
[29] S.M. Porritt, P.C. Cropper, L. Shao, C.I. Goodier, Ranking of interventions to reduce dwelling overheating during heat waves, Energy and Buildings 55(0) (2012) 16-27.
[30] E. Oikonomou, M. Davies, A. Mavrogianni, P. Biddulph, P. Wilkinson, M. Kolokotroni, Modelling the relative importance of the urban heat island and the thermal quality of dwellings for overheating in London, Building and Environment 57(0) (2012) 223-238.
[31] J. Taylor, P. Wilkinson, M. Davies, B. Armstrong, Z. Chalabi, A. Mavrogianni, P. Symonds, E. Oikonomou, S.I. Bohnenstengel, Mapping the effects of urban heat island, housing, and age on excess heat-related mortality in London, Urban Climate 14, Part 4 (2015) 517-528.
[32] C. Liu, T. Kershaw, M.E. Eames, D.A. Coley, Future probabilistic hot summer years for overheating risk assessments, Building and Environment 105 (2016) 56-68.
[33] ONS, 2011 Census Ward Profile No.4 – Housing and Accommodation, Office for National Statistics, UK, 2011.
[34] J. Holden, R. Rose, Temperature and surface lapse rate change: a study of the UK's longest upland instrumental record, International Journal of Climatology 31(6) (2011) 907-919.
[35] URBED, Sheffield Garden City? Options for long term urban growth, Urbanism, Environment and Design, UK, 2015.
[36] S.E. Belcher, J.N. Hacker, D.S. Powell, Constructing design weather data for future climates, Building Services Engineering Research and Technology 26(1) (2005) 49-61.
[37] P.D. Jones, C.G. Kilsby, C. Harpham, V. Glenis, A. Burton, UK Climate Projections science report: Projections of future daily climate for the UK from the Weather Generator, University of Newcastle, UK University of Newcastle, UK 2010.
[38] G.J. Jenkins, J.M. Murphy, D.S. Sexton, J.A. Lowe, P. Jones, C.G. Kilsby, UK Climate Projections: Briefing Report, Met Office Hadley Centre, Exeter, UK, 2009.
[39] M. Eames, T.J. Kershaw, D. Coley, A comparison of future weather created from morphed observed weather and created by a weather generator, Building and Environment 56 (2012) 252-264.
[40] M. Eames, T. Kershaw, D. Coley, On the creation of future probabilistic design weather years from UKCP09, Building Services Engineering Research and Technology 32(2) (2011) 127-142.
[41] R. Watkins, G. Levermore, J. Parkinson, Constructing a future weather file for use in building simulation using UKCP09 projections, Building Services Engineering Research and Technology 32(3) (2011) 293-299.
[42] R. Watkins, G. Levermore, J. Parkinson, The design reference year - a new approach to testing a building in more extreme weather using UKCP09 projections, Building Services Engineering Research and Technology 34(2) (2012) 165-176.

[43] S.T. Smith, V. Hanby, Methodologies for the generation of design summer years for building energy simulation using UKCP09 probabilistic climate projections, Building Services Engineering Research and Technology 33(1) (2012) 9-17.
[44] M.F. Jentsch, M.E. Eames, G.J. Levermore, Generating near-extreme Summer Reference Years for building performance simulation, Building Services Engineering Research and Technology 36 (2015) 701-727.
[45] A. Mylona, The use of UKCP09 to produce weather files for building simulation, Building Services Engineering Research and Technology 33 (2012) 13.
[46] P. Hoppe, The physiological equivalent temperature - a universal index for the biometeorological assessment of the thermal environment, International journal of biometeorology 43(2) (1999) 71-5.
[47] Google, Map of Sheffield, 2017. The interactive map of UKCP09 User Interface http://ukclimateprojections-ui.metoffice.gov.uk/ui/req_bldr/location.php. (Accessed 10 Feb 2017).
[48] A.P. Ramallo-González, Vellei, M., Brown, M., Coley, D., A remote window surveying tool for energy efficient refurbishment, 6th International building Physics Conference, Turin, Italy, 2015.
[49] P. Littlefair, Daylight, sunlight and solar gain in the urban environment, Solar Energy 70(3) (2001) 177-185.
[50] EST, Cavity and solid walls, 2016. http://www.energysavingtrust.org.uk/home-insulation/cavity-wall. (Accessed 10/10 2016).
[51] NEA, Small-Sample Techniques, The National Education Association Bulletin 38 (1960) 99.
[52] The Research Advisors, Required Sample Size, 2006. http://research-advisors.com/tools/SampleSize.htm. (Accessed 6 July 2016).
[53] E. Allen, A. Pinney, Standard dwellings for modelling: details of dimensions, construction and occupancy schedules, Building Environmental Performance Analysis Club Watford, ND1990.
[54] DCLG, English Housing Survey Headline Report 2014-15, Department for Communities and Local Government, London, UK, 2016.
[55] C. Liu, Details for thermal modelling of typical UK dwellings, Data in Brief (2017).
[56] A. Beizaee, K.J. Lomas, S.K. Firth, National survey of summertime temperatures and overheating risk in English homes, Building and Environment 65(0) (2013) 1-17.
[57] Building Regulation 2010, Approved Document F, Ventilation. https://www.gov.uk/government/uploads/system/uploads/attachment_data/file/468871/ADF_LOCKED.pdf. (Accessed 20/11 2016).
[58] I. Richardson, M. Thomson, Domestic electricity demand model, Centre for Renewable Energy Systems Technology, Department of Electronic and Electrical Engineering, Loughborough University, Leicestershire LE11 3TU, UK, 2010.
[59] CIBSE, CIBSE Guide A: Environmental Design, The Chartered Institution of Building Services Engineers, London, 2006.
[60] CIBSE, CIBSE TM 49: Design Summer Years for London, The Chatered Institution of Building Services Engineers, London, 2014.
[61] B.G. Armstrong, Z. Chalabi, B. Fenn, S. Hajat, S. Kovats, A. Milojevic, P. Wilkinson, Association of mortality with high temperatures in a temperate climate: England and Wales, Journal of Epidemiology and Community Health 65(4) (2011) 340-345.
[62] ONS, Neighbourhood Statistics, in: Office for National Statistics (Ed.) London, UK, 2011.
[63] D. Coley, T. Kershaw, Changes in internal temperatures within the built environment as a response to a changing climate, Building and Environment 45(1) (2010) 89-93.